Available online at www.sciencedirect.com
SCIENCE DIRECT
Journal of Sound and Vibration 295 (2006) 194–213
JOURNAL OF SOUND AND VIBRATION
www.elsevier.com/locate/jsvi

Vibration of rings on a general elastic foundation

Xionghua Wu, Robert G. Parker*

Department of Mechanical Engineering, The Ohio State University, Columbus, OH 43202, USA

Received 22 July 2005; received in revised form 30 November 2005; accepted 2 January 2006
Available online 10 March 2006

Abstract

The free vibration eigensolutions of a thin ring on a general elastic foundation are obtained by perturbation and Galerkin analyses. Natural frequencies and vibration modes are determined as closed-form expressions for a ring having a circumferentially varying foundation of very general description. The elastic foundation consists of two orthogonal distributed springs oriented at an arbitrary inclination angle. The foundation stiffnesses vary circumferentially. The simple eigensolution expressions explicitly show the parameter dependencies, lead to natural frequency splitting rules for degenerate unperturbed eigenvalues at both first and second orders of perturbation, and identify which nodal diameter Fourier components contaminate a given n nodal diameter base mode of the free ring. Discrete spring supports are treated as a special case where the natural frequencies are determined by five parameters: nondimensional spring stiffness, stiffness angle, support angle, number of springs, and location of the springs. The predicted effects of these parameters on the natural frequencies are verified numerically. As an application and as the motivating problem for the study, the natural frequencies and vibration modes of a ring gear used in helicopter planetary gears with unequally spaced planets are investigated.

1. Introduction

Structures having ring geometry are widely used in mechanical systems, such as gears, tires, bearings and rotors. For some purposes, these structures are modeled as rings with elastic spring connections to the mating components. This work is motivated by planetary gear systems, where the internal (or ring) gear is an elastic ring. Ring-planet gear tooth meshes are modeled as elastic springs due to tooth compliance [1,2]. These tooth meshes are not necessarily equally spaced and are inclined relative to the radial direction as tooth meshing occurs along the line of action. Planetary gears used in helicopters and aircraft engines usually have thin ring gears, justifying use thin ring theory. From a power density point of view, the ring gear must be thin to reduce weight, and a thin ring introduces compliance that improves load sharing among the planets [3–5]. Kahraman et al. [6] verified the importance of ring gear compliance when they computationally studied the vibration of a planetary gear used in an automotive transmission.

*Corresponding author. Tel.: +614 688 3922; fax: +614 292 3163.
E-mail address: parker.242@osu.edu (R.G. Parker).

0022-460X/$ - see front matter © 2006 Elsevier Ltd. All rights reserved.
doi:10.1016/j.jsv.2006.01.007

Nomenclature

α	stiffness angle
β	support angle
ε	nondimensional stiffness
γ	modulation angle
ν	Poisson ratio
θ_j	location of the jth support
ρ	mass density per unit length
τ	nondimensional time
ω	nondimensional natural frequencies
E	Young's modulus
F_t	tangential force per unit length
F_r	radial force per unit length
J	area moment of inertia
M_{11}	bending moment
N_{11}	axial force
N	number of Galerkin expansion terms
Q_{13}	shear force
K	stiffness per unit length
l	number of supports
n	mode number
r	radius of neutral axis
t	time
u	tangential displacement
u^*	nondimensional displacement
w	radial displacement

The ring vibration literature contains a variety of approaches for analyzing the influence of supports. Rao and Sundararajan [7] investigated the natural frequencies and vibration modes of rings on rigid radial supports by separating the ring into several parts with supports located at the ends of each segment. This method is cumbersome for cases with many supports. Sahay and Sundararajan [8] developed a method that can be applied to rings having many springs but with the limitation that cyclic symmetry is required. Many other methods such as the complementary transfer matrix method [9], transfer matrix method [10,11] and wave approach [12] have been applied to investigate vibration characteristics of rings on multiple radial springs supports. Detinko [13] investigated the free vibration of a thick ring on multiple radial springs by the Galerkin method, where the extension of the neutral axis, shear deformation and rotary inertia are considered. The effect of these factors on natural frequencies is negligible for thin rings. In Detinko's paper, the springs do not have to be equally spaced but need at least one axis of symmetry. Most of the above works restrict their studies to the problem of rings with discrete radial springs. In this paper, the distributed elastic foundation is more general.

When a structure deviates from axisymmetry, its natural frequencies and vibration modes can change significantly. This attracted many researchers to investigate problems of axisymmetric structures with asymmetric features. The asymmetries may come from manufacturing errors, dimensional variations, material nonuniformity, or attached masses and springs. Allaei et al. [14] analyzed the natural frequencies and vibration modes of a ring with radial spring attachments. They formulated the characteristic equation by the receptance method, obtained natural frequencies from the roots of the characteristic equation, and achieved mode shapes by the mode expansion method. Yu and Mote [15] studied the effects of radial slots of circular plates with rotating load and provided a rule for natural frequency splitting in circular plates with equally spaced, identical radial slots. Tseng and Wickert [16] studied the vibration of an eccentrically clamped annular plate and pointed out splitting of the degenerate natural frequencies. Parker and Mote [17–19] used perturbation analysis to investigate the eigensolutions for plate vibration and the wave equation on annular domains with boundary shape or stiffness variations. Natural frequency splitting rules were generalized to arbitrary distributed asymmetric deviations. Kim et al. [20] presented a natural frequency splitting rule for general rotationally periodic structures and investigated the effects of imperfection on both repeated and split natural frequency modes. A natural frequency splitting rule and a mode contamination rule for axisymmetric structures with identical, evenly spaced asymmetries were obtained by Chang and Wickert [21,22] when they studied the vibration of rotationally periodic structures.

This work investigates the dynamic characteristics of rings with asymmetry from an attached elastic foundation through perturbation and Galerkin methods. General rules of natural frequency splitting and mode contamination are obtained, and the vibration properties are examined for changes in the major parameters.

2. Mathematical formulation

Fig. 1 shows a thin ring with two perpendicular distributed foundations: one has stiffness $kd(\theta)$ and the other has stiffness $ke(\theta)$, where k is a dimensional stiffness, and $d(\theta)$ and $e(\theta)$ are dimensionless O(1) stiffness distribution functions. To retain full generality, the foundation at each circumferential location is oriented at an arbitrary inclination angle β with the radial direction. This permits natural application to planetary gears where tooth meshing occurs along the line of action defined by the pressure angle, and the ring gear may be supported on its outside by angled spline teeth. From in-plane force and moment balances of this ring segment and the constitutive relation, one obtains the equations (Fig. 2)

$$\rho r\ddot{u}\,\mathrm{d}\theta - \frac{\partial N_{11}}{\partial\theta}\,\mathrm{d}\theta - Q_{13}\,\mathrm{d}\theta - F_t r\,\mathrm{d}\theta = 0, \tag{1}$$

$$\rho r\ddot{w}\,\mathrm{d}\theta - \frac{\partial Q_{13}}{\partial\theta}\mathrm{d}\theta + N_{11}\,\mathrm{d}\theta - F_r r\,\mathrm{d}\theta = 0, \tag{2}$$

$$\frac{\partial M_{11}}{r\partial\theta} = Q_{13}, \quad M_{11} = \frac{EJ}{1-\nu^2}\left(\frac{\partial u}{r^2\partial\theta} - \frac{\partial^2 w}{r^2\partial\theta^2}\right), \tag{3}$$

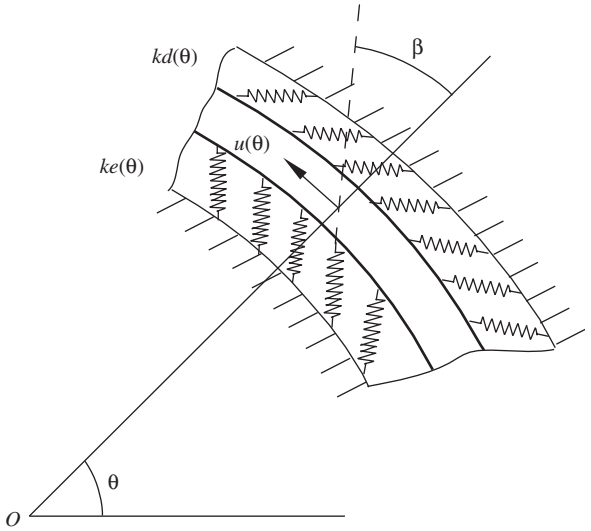

Fig. 1. Ring vibration with elastic foundation.

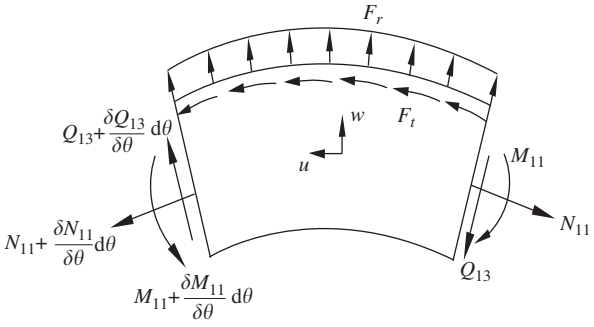

Fig. 2. Ring segment.

where $u(\theta, t)$ is the tangential displacement. The elastic foundation appears through the F_r and F_t terms. For inextensible in-plane vibration u and w are related by the constraint [23]

$$\frac{\partial u}{\partial \theta} + w = 0. \tag{4}$$

Eqs. (1)–(4) yield the equation of motion

$$\rho \frac{\partial^2}{\partial t^2}\left(u - \frac{\partial^2 u}{\partial \theta^2}\right) - \frac{EJ}{r^4(1-\nu^2)}\left(\frac{\partial^6 u}{\partial \theta^6} + 2\frac{\partial^4 u}{\partial \theta^4} + \frac{\partial^2 u}{\partial \theta^2}\right) = F_t + \frac{\partial F_r}{\partial \theta}. \tag{5}$$

The tangential and radial distributed forces F_t and F_r are:

$$\mathbf{F} = -\mathbf{T}^{-1}\mathbf{K}\mathbf{T}\mathbf{x}, \tag{6}$$

$$\mathbf{F} = \begin{bmatrix} F_t \\ F_r \end{bmatrix}, \quad \mathbf{T} = \begin{bmatrix} \cos\beta & -\sin\beta \\ \sin\beta & \cos\beta \end{bmatrix}, \quad \mathbf{K} = \begin{bmatrix} kd(\theta) & 0 \\ 0 & ke(\theta) \end{bmatrix}, \quad \mathbf{x} = \begin{bmatrix} u \\ w \end{bmatrix}. \tag{7}$$

Introducing dimensionless quantities by the definitions

$$u^* = \frac{u}{r}, \quad \tau = \frac{t}{T}, \quad T = \sqrt{\frac{\rho r^4(1-\nu^2)}{EJ}}, \quad f_t = \frac{r^4(1-\nu^2)F_t}{EJ}, \quad f_r = \frac{r^4(1-\nu^2)F_r}{EJ}, \quad \varepsilon = \frac{kr^3(1-\nu^2)}{EJ}, \tag{8}$$

where ε is the dimensionless foundation stiffness, the equation of motion is

$$Mu^*_{\tau\tau} + Lu^* + \varepsilon L_1 u^* = 0, \tag{9}$$

$$M = 1 - \frac{\partial^2}{\partial \theta^2}, \quad L = -\left(\frac{\partial^6}{\partial \theta^6} + 2\frac{\partial^4}{\partial \theta^4} + \frac{\partial^2}{\partial \theta^2}\right), \quad L_1 = g + \frac{\mathrm{d}h}{\mathrm{d}\theta} - q\frac{\partial^2}{\partial \theta^2} - \frac{\mathrm{d}q}{\mathrm{d}\theta}\frac{\partial}{\partial \theta}, \tag{10}$$

$$g(\theta) = d(\theta)\cos^2\beta + e(\theta)\sin^2\beta, \tag{11}$$

$$h(\theta) = [e(\theta) - d(\theta)]\sin\beta\cos\beta, \quad q(\theta) = d(\theta)\sin^2\beta + e(\theta)\cos^2\beta. \tag{12}$$

The operators L and M are self-adjoint with the inner product $<u, v> = \int_0^{2\pi} u\tilde{v}\,\mathrm{d}\theta$, with $\sim$ denoting complex conjugate. In what follows the superscript * on u^* is omitted.

2.1. Perturbation method

With the solution $u(\theta, t) \to u(\theta)\mathrm{e}^{\mathrm{i}\omega t}$, the eigenvalue problem of (9) is

$$Lu - \omega^2 Mu = -\varepsilon L_1 u. \tag{13}$$

When the foundation stiffness is small compared to the ring bending stiffness, $\varepsilon << 1$, the perturbed eigensolutions u_n and ω_n^2 are represented as asymptotic expansions in ε:

$$u_n = \bar{u}_n + \varepsilon v_n + \varepsilon^2 \eta_n + \mathrm{O}(\varepsilon^3), \tag{14}$$

$$\omega_n^2 = \bar{\omega}_n^2 + \varepsilon\lambda_n + \varepsilon^2\gamma_n + \mathrm{O}(\varepsilon^3). \tag{15}$$

Substitution of Eqs. (14) and (15) into Eq. (13) generates the sequence of perturbation problems

$$L\bar{u}_n - \bar{\omega}_n^2 M\bar{u}_n = 0, \tag{16}$$

$$Lv_n - \bar{\omega}_n^2 Mv_n = -L_1\bar{u}_n + \lambda_n M\bar{u}_n, \tag{17}$$

$$L\eta_n - \bar{\omega}_n^2 M\eta_n = -L_1 v_n + \lambda_n Mv_n + \gamma_n M\bar{u}_n. \tag{18}$$

The bending natural frequencies $\bar{\omega}_n$ of a free ring are degenerate with multiplicity two. These and the associated n nodal diameter unperturbed eigenfunctions that satisfy Eq. (16) are

$$\bar{\omega}_n = \sqrt{\frac{n^2(n^2-1)^2}{n^2+1}}, \quad \bar{u}_{n,1} = \frac{1}{\sqrt{2\pi(1+n^2)}} e^{in\theta}, \quad \bar{u}_{n,2} = \frac{1}{\sqrt{2\pi(1+n^2)}} e^{-in\theta}, \tag{19}$$

where $<\bar{u}_{n,i}, \ M\bar{u}_{n,j}> = \delta_{ij}$. The general unperturbed eigenfunction $\bar{u}_n$ of Eq. (16) is a linear combination of $\bar{u}_{n,1}$ and $\bar{u}_{n,2}$:

$$\bar{u}_n = a_{n,1}\bar{u}_{n,1} + a_{n,2}\bar{u}_{n,2} \tag{20}$$

where $a_{n,1}$ and $a_{n,2}$ are determined subsequently to ensure continuous change in u_n of Eq. (14) as $\varepsilon \to 0$. For the self-adjoint problems (17) and (18) the solvability conditions are

$$< -L_1\bar{u}_n + \lambda_n M\bar{u}_n, \bar{u}_{n,i}> = 0, \quad i = 1,2, \tag{21}$$

$$< -L_1 v_n + \lambda_n M v_n + \gamma_n M\bar{u}_n, \bar{u}_{n,i}> = 0, \quad i = 1,2. \tag{22}$$

With the normalization condition $<Mu_n, u_n> = 1$, Eq. (20) and the solvability conditions (21) form the algebraic eigenvalue problem

$$\mathbf{D}\mathbf{a}_n = \lambda_n \mathbf{a}_n, \tag{23}$$

$$\mathbf{D} = \frac{1}{1+n^2}\begin{bmatrix} g_0 + n^2 q_0 & g_{2n} + i2nh_{2n} - n^2 q_{2n} \\ g_{-2n} - i2nh_{-2n} - n^2 q_{-2n} & g_0 + n^2 q_0 \end{bmatrix}, \quad \mathbf{a}_n = \begin{pmatrix} a_{n,1} \\ a_{n,2} \end{pmatrix}. \tag{24}$$

where g_m, h_m and q_m in Eq. (24) are from the Fourier expansions

$$g(\theta) = \sum_{m=-\infty}^{\infty} g_m e^{im\theta}, \quad h(\theta) = \sum_{m=-\infty}^{\infty} h_m e^{im\theta}, \quad q(\theta) = \sum_{m=-\infty}^{\infty} q_m e^{im\theta}, \tag{25}$$

$$g_m = d_m \cos^2\beta + e_m \sin^2\beta, \ h_m = (e_m - d_m)\sin\beta\cos\beta, \ q_m = d_m \sin^2\beta + e_m \cos^2\beta, \tag{26}$$

and d_m, e_m are the complex Fourier coefficients of $d(\theta)$ and $e(\theta)$. $\mathbf{D}$ is Hermitian. Solution of the eigenvalue problem for $\mathbf{D}$ gives the first-order eigenvalue perturbations in Eq. (14) as

$$\begin{matrix} \lambda_{n,1} \\ \lambda_{n,2} \end{matrix} = \frac{1}{1+n^2}\left[d_0(\cos^2\beta + n^2\sin^2\beta) + e_0(\sin^2\beta + n^2\cos^2\beta)\right] \pm \frac{1}{1+n^2}\left|d_{2n}(\cos\beta - in\sin\beta)^2 + e_{2n}(\sin\beta + in\cos\beta)^2\right|. \tag{27}$$

If $\mathbf{D}$ has distinct eigenvalues $\lambda_{n,1} \neq \lambda_{n,2}$, the degenerate unperturbed eigenvalues split. The two eigenvectors $\mathbf{a}_n$ in Eq. (24) are then determined following the normalization $<Mu_n, u_n> = 1$. This establishes $a_{n,1}$ and $a_{n,2}$ for each mode (20) of the split natural frequencies, and the unperturbed eigenfunctions $\bar{u}_n$ are determinate at the first order. If $\mathbf{D}$ has repeated eigenvalues $\lambda_{n,1} = \lambda_{n,2}$, however, the perturbed eigenvalues do not split at this order of perturbation, any $\mathbf{a}_n$ satisfies Eq. (24), and the unperturbed eigenfunctions $\bar{u}_n$ in Eq. (20) remain indeterminate.

The n nodal diameter natural frequencies split at first order if the second term of Eq. (27) is nonzero; otherwise they remain repeated. Obviously, the n nodal diameter natural frequencies remain repeated for $d_{2n} = e_{2n} = 0$. If one or both of d_{2n} and e_{2n} are non-zero, the natural frequencies split at first order except when d_{2n} and e_{2n} satisfy

$$d_{2n}(\cos\beta - in\sin\beta)^2 + e_{2n}(\sin\beta + in\cos\beta)^2 = 0. \tag{28}$$

In these cases (an example is given later), the natural frequencies split if either of the individual distribution are present separately but remain repeated with both distributed springs acting simultaneously.

Repeated and split natural frequencies experience different influence from the asymmetry. The impact on some of the split natural frequencies is larger than on the repeated natural frequencies. The sum of the

first-order eigenvalue perturbations for an arbitrary eigenvalue pair is

$$\lambda_{n,1}+\lambda_{n,2}=2\left[d_0(\cos^2\beta+n^2\sin^2\beta)+e_0(\sin^2\beta+n^2\cos^2\beta)\right]/(1+n^2). \tag{29}$$

For a split natural frequency pair, one natural frequency changes less than $\varepsilon(\lambda_{n,1}+\lambda_{n,2})/(4\bar{\omega}_n)$, and the other one changes more. A limit case is a ring having equally spaced supports with one spring in each support. In that case, the natural frequency change is maximal for one split natural frequency while it is zero for the other. Natural frequencies that remain repeated always change by $\varepsilon\lambda_{n,1}/(2\bar{\omega}_n)=\varepsilon\lambda_{n,2}/(2\bar{\omega}_n)$.

The first-order eigenfunction perturbation v_n governed by Eq. (17) is expanded as a series of the complete unperturbed eigenfunctions

$$v_n=\sum_{s=-\infty}^{\infty} r_{n,s}e^{is\theta}=\sum_{s=-\infty,s\neq\pm n}^{\infty} r_{n,s}e^{is\theta}+r_{n,n}e^{in\theta}+r_{n,-n}e^{-in\theta}. \tag{30}$$

Substituting Eq. (30) into Eq. (17) and forming the inner product of Eq. (17) with $e^{im\theta}$ yields

$$r_{n,s}=\sqrt{\frac{1+n^2}{2\pi}}C_{n,s}(P_{n,s}a_{n,1}+P_{-n,s}a_{n,2}),\quad C_{n,s}=\frac{1}{(1+n^2)(\bar{\omega}_n^2-\bar{\omega}_s^2)(1+s^2)},\quad s\neq\pm n, \tag{31}$$

$$P_{n,s}=d_{s-n}(\cos\beta+in\sin\beta)(\cos\beta-is\sin\beta)+e_{s-n}(\sin\beta-in\cos\beta)(\sin\beta+is\cos\beta). \tag{32}$$

The coefficients $r_{n,n}$ and $r_{n,-n}$ remain indeterminate from this process because the inner product of the left and right sides of Eq. (17) with $e^{\pm in\theta}$ vanish (one must use $\lambda_n\mathbf{a}_n=\mathbf{D}\mathbf{a}_n$ from Eq. (23) to show the right sides vanishes). Indeed, $r_{n,n}$ and $r_{n,-n}$ are governed by the normalization condition $<M\bar{u}_n,v_n>=0$ as

$$a_{n,1}r_{n,n}+a_{n,2}r_{n,-n}=0. \tag{33}$$

For eigenvalues that split at first order, $r_{n,n}$ and $r_{n,-n}$ are determined by Eq. (33) and the solvability conditions (22) of the second-order perturbation equation (18). These equations form the Hermitian algebraic problem

$$\begin{bmatrix} -P_{n,n}+(1+n^2)\lambda_n & -P_{-n,n} & \sqrt{\frac{1+n^2}{2\pi}}a_{n,1} \\ -P_{n,-n} & -P_{n,n}+(1+n^2)\lambda_n & \sqrt{\frac{1+n^2}{2\pi}}a_{n,2} \\ \sqrt{\frac{1+n^2}{2\pi}}a_{n,1} & \sqrt{\frac{1+n^2}{2\pi}}a_{n,2} & 0 \end{bmatrix}\begin{bmatrix} r_{n,n} \\ r_{n,-n} \\ \gamma_n \end{bmatrix}=\begin{bmatrix} \sum_{s\neq\pm n} P_{s,n}r_{n,s} \\ \sum_{s\neq\pm n} P_{s,-n}r_{n,s} \\ 0 \end{bmatrix}, \tag{34}$$

Because $a_{n,1}$ and $a_{n,2}$ are known when the eigenvalues split at first-order perturbation, two solutions for $r_{n,n}$, $r_{n,-n}$ and γ_n are obtained from Eq. (34) for the two eigensolutions of Eq. (23).

For eigenvalues that remain degenerate at first order, $a_{n,1}$ and $a_{n,2}$ are arbitrary. This and Eq. (33) yield $r_{n,n}=r_{n,-n}=0$. The solvability conditions of Eq. (22) generate an algebraic eigenvalue problem for γ_n:

$$\mathbf{E}\mathbf{a}_n=\gamma_n\mathbf{a}_n, \tag{35}$$

$$\mathbf{E}=\begin{bmatrix} \sum_{s=-\infty,s\neq\pm n}^{\infty} C_{n,s}P_{n,s}P_{s,n} & \sum_{s=-\infty,s\neq\pm n}^{\infty} C_{n,s}P_{-n,s}P_{s,n} \\ \sum_{s=-\infty,s\neq\pm n}^{\infty} C_{n,s}P_{n,s}P_{s,-n} & \sum_{s=-\infty,s\neq\pm n}^{\infty} C_{n,s}P_{-n,s}P_{s,-n} \end{bmatrix}, \tag{36}$$

where $P_{s,n}$ is the complex conjugate of $P_{n,s}$. The eigenvalues of Eq. (36) yield the second-order eigenvalue perturbations γ_n:

$$\gamma_n=\sum_{s=-\infty,s\neq\pm n}^{\infty} C_{n,s}\left|P_{n,s}\right|^2\pm\left|\sum_{s=-\infty,s\neq\pm n}^{\infty} C_{n,s}P_{-n,s}P_{s,n}\right|. \tag{37}$$

The properties of $P_{-n,s}P_{s,n}$, which is governed by the foundation's Fourier coefficients d_m and e_m, dictate whether the natural frequencies split at second-order perturbation. The properties of $P_{-n,s}P_{s,n}$ for identical,

equally spaced discrete supports are obtained in Appendix A; these guarantee that all eigenvalues that are degenerate at first order remain degenerate for higher order perturbations.

The closed-form eigenfunction approximation is

$$u_n = a_{n,1}\bar{u}_{n,1} + a_{n,2}\bar{u}_{n,2} + \varepsilon \sum_{s=-\infty}^{\infty} r_{n,s} e^{is\theta}. \tag{38}$$

Because of asymmetry from the circumferentially varying elastic foundation, the vibration modes no longer consist of pure n nodal diameter sinusoidal variations as they do for a free ring. The base n nodal diameter mode (or unperturbed eigenfunction (20)) is contaminated by additional nodal diameter components. The last term in Eq. (38) governs how the elastic foundation introduces s nodal diameter contaminants into an unperturbed n nodal diameter base mode. The coefficients $r_{n,s}$ in Eq. (31) determine the presence and magnitude of each contaminant for given base mode and asymmetric foundation $e(\theta)$ and $d(\theta)$. These contaminants can change the dynamic characteristics, and especially the forced response, dramatically. The mode contamination rule states: an n nodal diameter base mode will be contaminated with the s nodal diameter component if s satisfies

$$s \pm n = p, \tag{39}$$

where p is any index (positive or negative) of nonzero complex Fourier coefficients for either of the foundation stiffness distribution functions $d(\theta)$ and $e(\theta)$. The s nodal diameter component will disappear, however, for the unusual case where one or more of $d_{s\pm n}$ and $e_{s\pm n}$ are nonzero but occur such that $r_{n,s} = 0$. The ascending sequence of all nodal diameter components for a given n nodal diameter base mode is called the contamination sequence for that mode.

2.2. Galerkin method

An alternative solution spatially discretizes Eq. (9) by expanding u as a series of basis functions $u(\theta,\tau) = \sum_{n=N}^{N} U_n(\tau)e^{in\theta}$. Galerkin discretization yields

$$(1+n^2)\ddot{U}_n + n^2(n^2-1)^2 U_n + \varepsilon \sum_{m=-N}^{N} [g_m + n(n-m)q_n + imh_m]U_m = 0. \tag{40}$$

The matrix form of Eq. (40) and the associated eigenvalue problem are

$$\mathbf{M}\ddot{\mathbf{U}} + (\mathbf{\Psi} + \boldsymbol{\lambda})\mathbf{U} = \mathbf{0}, \quad -\omega^2\mathbf{M}\mathbf{v} + (\mathbf{\Psi} + \boldsymbol{\lambda})\mathbf{v} = \mathbf{0}, \tag{41}$$

$$\mathbf{M} = \mathrm{diag}[1+n^2], \quad \mathbf{\Psi} = \mathrm{diag}[n^2(n^2-1)^2], \tag{42}$$

$$\lambda_{n+N+1,m+N+1} = \varepsilon[g_m + n(n-m)q_n + imh_m], \quad m,n = -N,\ldots,N. \tag{43}$$

For identical, equally spaced springs with no inclination ($\beta = 0$), one has

$$d(\theta) = \sin\alpha \sum_{i=1}^{l} \delta(\theta - \psi_i), \quad e(\theta) = \cos\alpha \sum_{i=1}^{l} \delta(\theta - \psi_i). \tag{44}$$

$$\psi_i = 2\pi(i-1)/l, \quad i = 1,\ldots,l, \tag{45}$$

where α is a stiffness angle that can be varied to change the relative stiffness between $d(\theta)$ and $e(\theta)$. In this case Eq. (40) simplifies to

$$(1+n^2)\ddot{U}_n + n^2(n^2-1)^2 U_n + \frac{\varepsilon}{2\pi} \sum_{m=-N}^{N} U_m(\sin\alpha + mn\cos\alpha) \sum_{i=1}^{l} e^{i(m-n)\theta} = 0,\ m,n = -N,\ldots,N. \tag{46}$$

For a planetary ring gear, β is no longer zero. Each ring-planet gear tooth mesh with pressure angle φ is modeled as a single spring with $\alpha = \pi/2$ and $\beta = \pi/2 - \varphi$.

3. Method validation

Fig. 3 shows the natural frequencies of a ring with four equally spaced radial springs obtained by perturbation and Galerkin discretization. For a wide range of nondimensional spring stiffness ε, the natural frequencies match well with differences less than 1%.

The vibration of free rings having two identical, equally spaced springs has been investigated by prior researchers [10–13]. The problem is briefly considered to confirm the accuracy and convergence of the numerical method. Table 1 gives the natural frequencies of a ring having two radial springs located at 0 and π. The results with $N = 50$ are compared with those of Ref. [10], where N is the number of Galerkin expansion terms. Some natural frequencies, such as ω_2,ω_4,ω_6, match very well for a wide range of ε, but others do not. When the radial springs are identical and equally spaced there always exist some natural frequencies that are independent of spring stiffness due to all the springs being located at nodes of these modes. They are also

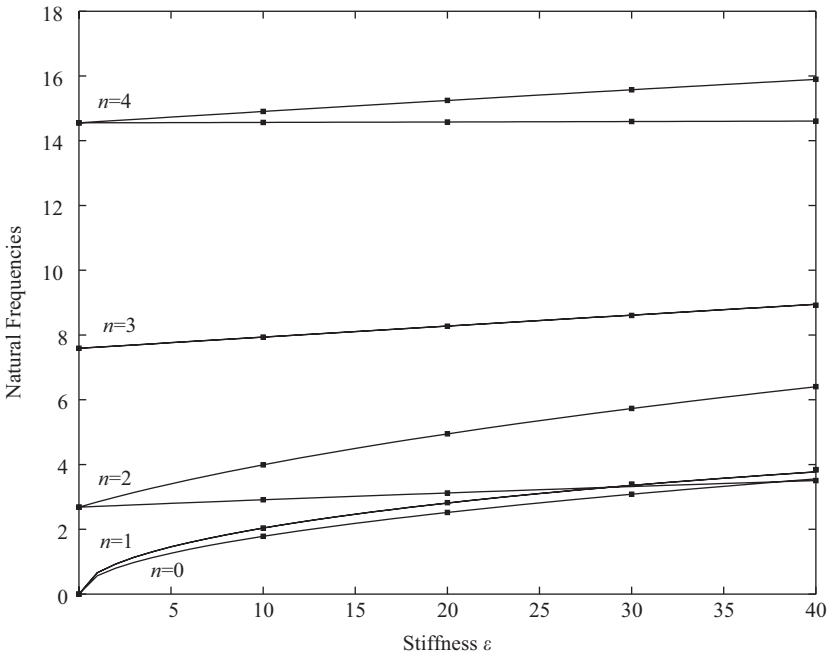

Fig. 3. Natural frequencies of rings having four equally spaced radial springs. The symbols denote values calculated by the Galerkin method; solid lines denote results from perturbation.

Table 1
Nondimensional natural frequencies of a ring with two identical, equally spaced, radial springs compared to values from Ref. [10]

ε	1 nodal diameter				2 nodal diameter				3 nodal diameter			
	ω_1	ω_1 [10]	ω_2	ω_2 [10]	ω_3	ω_3 [10]	ω_4	ω_4 [10]	ω_5	ω_5 [10]	ω_6	ω_6 [10]
0	0	—	0	—	2.6833	—	2.6833	—	7.5895	—	7.5895	—
0.1	0	—	0.1783	0.1779	2.6833	4.3843	2.6928	2.6928	7.5895	9.6542	7.5932	7.5933
1	0	—	0.5609	0.5610	2.6833	4.3843	2.7762	2.7762	7.5895	9.6542	7.6273	7.6283
10	0	—	1.6854	1.6854	2.6833	4.3845	3.4792	3.4792	7.5895	9.6615	7.9702	7.9706
100	0	—	3.6071	3.6071	2.6833	4.3844	6.5267	6.5279	7.5895	9.6449	10.935	10.915
600	0	—	4.2364	4.2359	2.6833	4.3845	8.9087	8.9090	7.5895	9.6511	15.868	—
∞	0	—	4.3844	4.385*	2.6833	—	9.6519	9.657*	7.5895	—	17.922	—

For $\varepsilon \to \infty$, results with * come from Ref. [13]. Note: (–) means no result is provided. $v = 0$ is assumed, so that ε is the same as in Ref. [10].

Table 2
Nondimensional natural frequencies of a ring with three identical, equally spaced radial springs compared to values from Ref. [13]

ε	1 nodal diameter			2 nodal diameter			3 nodal diameter			
	ω_1	ω_1 [13]	ω_2 [13]	ω_3, ω_4	ω_3 [13]	ω_4 [13]	ω_5	ω_5 [13]	ω_6	ω_6 [13]
0	0	0	0	2.6833	2.683	2.683	7.5895	7.589	7.5895	7.589
1	0.4750	0.4750	0.6012	2.7555	2.755	2.804	7.5895	7.589	7.6458	14.57
10	1.1871	1.187	1.330	3.4329	3.432	3.872	7.5895	7.589	8.1304	14.71
100	1.5855	1.586	1.606	6.9712	6.973	7.795	7.5895	7.589	11.614	16.08
1000	1.6378	1.638	1.640	9.9941	10.00	10.15	7.5895	7.589	19.605	19.61
∞	1.6437	1.644	1.644	10.465	10.47	10.47	7.5895	7.589	20.296	20.30

natural frequencies of the free ring. As revealed in Table 1, large discrepancies occur exactly for these natural frequencies. For instance, 2.6833 and 7.5895 are the two and three nodal diameter natural frequencies of a free ring without springs, as expected. In Ref. [10], however, the corresponding values are incorrectly given as 4.3843 and 9.6542, which are natural frequencies for two rigid radial springs (see ω_2 and ω_4 for $\varepsilon \to \infty$). The present results agree well with known results and previous research [13] for two special cases: one case is $\varepsilon \to 0$, which corresponds to rings with no springs; the other is $\varepsilon \to \infty$, which corresponds to rigid springs.

Natural frequencies of a ring with three identical, equally spaced radial springs are shown in Table 2 with comparisons to results in Ref. [13]. Many values agree well, although differences arise due to splitting of degenerate (repeated) natural frequencies. Published research about axisymmetric structures with identical, equally spaced asymmetries [14–18,20,22,24–26] ensure the following natural frequency splitting rule holds: when the nodal diameter n and the number of supports l satisfy $n = ml/2$ for even l or $n = ml$ for odd l ($m = 1,2,3\ldots$), then the degenerate natural frequencies split. The natural frequency splitting behavior for the present solution in Table 2 obeys this rule. When $l = 3$ the first and second pairs of natural frequencies are repeated, and the third pair of natural frequencies splits. Results in Ref. [13] violate this rule.

4. Vibration of rings with identical, equally spaced springs

The distributed elastic foundation modeled in this study encompasses a broad range of possibilities. Discrete spring supports are of primary interest because this work is motivated by planetary gear systems, where the ring gear is an elastic ring acted on by discrete ring-planet mesh stiffnesses.

4.1. Perturbation solution

For identical, equally spaced springs with no inclination ($\beta = 0$), the stiffness distribution functions are governed by Eq. (44). The Fourier coefficients of $d(\theta)$, $e(\theta)$ are

$$d_m = \begin{cases} 0 \\ l\sin\alpha/(2\pi) \end{cases}, e_m = \begin{cases} 0, & m/l \neq \text{int}, \\ l\cos\alpha/(2\pi), & m/l = \text{int}. \end{cases} \tag{47}$$

Two cases must be considered depending on the relationship between the base nodal diameter and the number of equally spaced springs.

Case 1: $2n/l \neq$ integer. Substituting Eq. (47) into Eq. (27), the first-order eigenvalue perturbations are repeated:

$$\lambda_{n,1} = \lambda_{n,2} = \frac{l(\sin\alpha + n^2\cos\alpha)}{2\pi(1+n^2)}. \tag{48}$$

The eigenvalues do not split at the first order perturbation. The eigenvectors $\mathbf{a}_n$ of $\mathbf{D}$ are arbitrary unit vectors. Substitution of Eq. (48) into Eqs. (30) and (31) yields the first-order eigenfunction perturbations

$$v_n = \frac{l}{2\pi}\sqrt{\frac{1+n^2}{2\pi}}\sum_{m=\pm1}^{\pm\infty}\{a_{n,1}C_{n,ml+n}[\sin\alpha + (n+ml)n\cos\alpha]e^{i(ml+n)\theta} + a_{n,2}C_{n,ml-n}[\sin\alpha + (n-ml)n\cos\alpha]e^{i(ml-n)\theta}\}, \tag{49}$$

where $a_{n,1}$ and $a_{n,2}$ are arbitrary. The second-order eigenvalue perturbations are obtained from the same substitution into Eq. (37):

$$\gamma_n = \sum_{m=\pm1}^{\pm\infty}\frac{l^2}{4\pi^2}C_{n,ml+n}[\sin\alpha + (ml+n)n\cos\alpha]^2. \tag{50}$$

Note that the second-order eigenvalue perturbation is calculated even though v_n in Eq. (49) is not fully determined as $\mathbf{a}_n$ is an arbitrary unit vector. The eigenvalues do not split at the second order either. In fact, the eigenvalues associated with the n nodal diameter base mode will not split at any order of perturbation for rings on equally spaced springs when $2n/l \neq$ integer, as shown in Appendix A.

Case 2: $2n/1 =$ integer. The eigenvalues split at the first-order. The eigensolutions at first order are

$$\lambda_{n,1} = \frac{l\sin\alpha}{\pi(1+n^2)}, \lambda_{n,2} = \frac{n^2 l\cos\alpha}{\pi(1+n^2)}, \quad \mathbf{a}_{n,1} = \frac{\sqrt{2}}{2}\begin{pmatrix}1\\1\end{pmatrix}, \quad \mathbf{a}_{n,2} = \frac{\sqrt{2}}{2}\begin{pmatrix}-1\\1\end{pmatrix}. \tag{51}$$

Substitution of Eqs. (51) and (31) into Eq. (34) yields $r_{n,n} = r_{n,-n} = 0$ for each split mode. In using Eq. (47) to reduce Eqs. (31) and (34) for this case, note that $(s-n)/l =$ integer if and only if $(s+n)/l =$ integer. The eigensolutions are

$$v_{n,1} = \sum_{m=-\infty,m\neq0,-2n/l}^{\infty}\frac{\sin\alpha}{2\pi}\sqrt{\frac{1+n^2}{\pi}}C_{n,ml+n}le^{i(ml+n)\theta}, \tag{52}$$

$$v_{n,2} = \sum_{m=-\infty,m\neq0,-2n/l}^{\infty}\frac{l\cos\alpha}{2\pi}\sqrt{\frac{1+n^2}{\pi}}C_{n,ml+n}(ml+n)ne^{i(ml+n)\theta}, \tag{53}$$

$$\gamma_{n,1} = \sum_{m=-\infty,m\neq0,-2n/l}^{\infty}\frac{l^2\sin\alpha}{2\pi^2}C_{n,n+ml}[\sin\alpha + (ml+n)n\cos\alpha], \tag{54}$$

$$\gamma_{n,2} = \sum_{m=-\infty,m\neq0,-2n/l}^{\infty}\frac{l^2\cos\alpha}{2\pi^2}C_{n,ml+n}(ml+n)n[\sin\alpha + (ml+n)n\cos\alpha]. \tag{55}$$

These expressions show the relationships between parameters and eigensolutions, which is convenient for modal analysis, system identification, response analyses and design.

The nonzero Fourier coefficient indices for equally spaced springs are integer multiples of the number of springs. Substitution of this into the general contamination rule (39) yields the mode contamination rule for rings having equally spaced springs:

$$|s \pm n| = ml, \quad m = 1,2,3,\ldots. \tag{56}$$

This rule is consistent with the mode contamination rule in previous works where discrete, equally spaced attachments are added to an axisymmetric structure [20–22]. The magnitude of each contaminating component is evident from Eqs. (49), (52) and (53).

Substitution of Eqs. (19) and (30) into Eq. (38) gives the expression for u_n:

$$u_n = (a_{n,1}+a_{n,2})\left[\sum_{s=1,s\neq n}^{\infty}A_s\cos s\theta + \cos n\theta\right] + i(a_{n,1}-a_{n,2})\left[\sum_{s=1,s\neq n}^{\infty}B_s\sin s\theta + \sin n\theta\right], \tag{57}$$

$$A_s = -\varepsilon\sqrt{\frac{1+n^2}{2\pi}}C_{n,s}(P_{n,s}+P_{n,-s}), \quad B_s = -\varepsilon\sqrt{\frac{1+n^2}{2\pi}}C_{n,s}(P_{n,s}-P_{n,-s}). \tag{58}$$

For repeated natural frequencies ($2n/l \neq int$), $\mathbf{a}_n$ are arbitrary unit vectors, and Eq. (57) is an arbitrary linear combination of the expressions in square brackets. Thus, one can regard the terms in the first square brackets as one mode of the degenerate pair and terms in the second square brackets as the other mode. For split natural frequencies, the two $\mathbf{a}_n$ are determinate, but substitution (separately) of $\mathbf{a}_n = \sqrt{2}/2(1,\ 1)^{\mathrm{T}}$ and $\mathbf{a}_n = \sqrt{2}/2(1,\ -1)^{\mathrm{T}}$ from Eq. (51) into Eq. (57) also yields the bracketed expressions in Eq. (57) as the modes. Thus, the bracketed expressions in Eq. (57) are the two vibration modes associated with the base n nodal diameter mode, regardless of whether the springs split the degenerate natural frequency. One mode is called the cos $n\theta$ mode and has only cosine components, while the other is called the sin $n\theta$ mode and has only sine components.

The distinction between the cases of splitting and no splitting lies in the properties of A_s and B_s, the coefficients of the contaminating components for the cos $n\theta$ and sin $n\theta$ modes. For no splitting of the degenerate unperturbed eigenvalues, the condition $2n/l \neq int$ guarantees $n-s$ and $-n-s$ cannot simultaneously be integer multiples of l because their difference is $2n$. This and Eq. (32) ensure either $P_{n,s}$ or $P_{n,-s}$ is zero. Therefore, if $s-n=ml$ ($P_{n,-s}=0$), then $A_s = B_s$. In contrast, if $s+n=ml$ ($P_{n,s}=0$), then $A_s = -B_s$. One of these two conditions holds. This structure of the base and contaminating Fourier coefficients for repeated natural frequencies does not hold when the natural frequencies split because both of $P_{n,s}$ and $P_{n,-s}$ are nonzero in Eq. (58).

As an example, the mode contamination properties are considered for a ring with five identical, equally spaced springs. Fig. 4(a) depicts the Galerkin method Fourier coefficients for the three nodal diameter mode, where the natural frequencies do not split. The mode contamination rule (57) is confirmed with the contaminants $s = 2, 7, 8, 12, 13\ldots$. Furthermore, the coefficients A_s and B_s satisfy $A_s = B_s$ for $s-n=ml$ and $A_s = -B_s$ for $s+n=ml$, as predicted by perturbation. In contrast, Fig. 4(b) shows the contamination

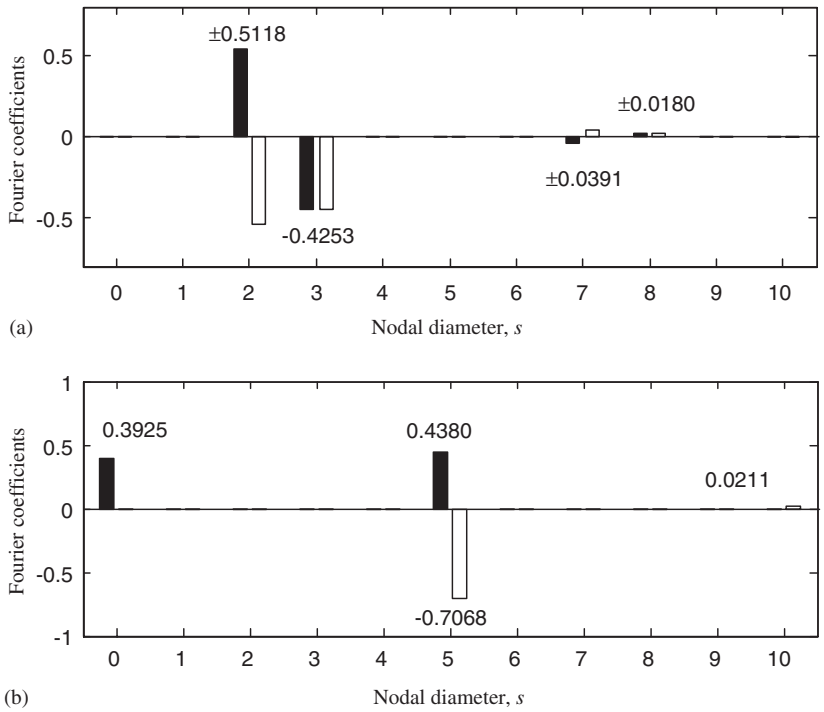

Fig. 4. Fourier coefficients of vibration modes for a ring with five identical, equally spaced springs with $\varepsilon = 500$, $\alpha = \pi/4$, $\beta = 0$. Black ■ (A_s) denotes the mode having cosine components, white □ (B_s) denotes the mode having sine components. (a) three nodal diameter modes; (b) five nodal diameter modes.

behavior of the five nodal diameter split natural frequency modes. Both the sine and cosine components of the fifth mode are contaminated by $s = 0, 10, 15, 20, \ldots$, but their magnitudes are different, as predicted. There is a special case for modes with split natural frequencies: when the discrete supports are uniform, equally spaced radial springs, only the cos $n\theta$ split modes are contaminated; the sin $n\theta$ split modes are associated with natural frequencies that are independent of the supports, so they have no contamination. On the contrary, cos $n\theta$ modes have no contamination for uniform, equally spaced tangential springs.

From $(\bar{\omega}_s^2 - \bar{\omega}_n^2)$ in the denominator of Eq. (31), the amplitude of a particular mode contamination component depends on the proximity $|s-n|$of the contaminating nodal diameter s to the base nodal diameter n. For repeated modes, the contaminations are prominent because the nodal diameters s of the contaminating components can be close to n. For split natural frequencies ω_n, however, the difference between s and n satisfies $|s-n| \geq l$, so $r_{n,s}$ is relatively small. Therefore, in what may seem a counter-intuitive result, split modes are less contaminated compared to repeated modes even though they have greater natural frequency change.

4.2. Mode classification for rings having identical, equally spaced spring supports

As shown in Appendix a for the case of identical, equally spaced spring supports, the natural frequency splitting rule does not change for the second or higher order perturbations. In other words, if a degenerate natural frequency does not split at first order, it does not split at any order. A similar conclusion exists for the mode contamination rule; the sets of nodal diameter components present in Eqs. (49), (52) and (53) do not change for the entire range of $\varepsilon > 0$. The modes of a ring having equally spaced springs are classified into distinct and degenerate modes as reduced from Eqs. (49), (52) and (53).

The distinct modes have distinct natural frequencies and reduce from Eqs. (52) and (53). They evolve from the n nodal diameter free ring modes where $2n/l =$ integer. They are linear combinations of the ml nodal diameter components, where $m = 0, 1, \ldots, \infty$:

$$(u^n)_1 = \sum_{m=0}^{\infty} U^n_{ml,1} \cos ml\theta, \quad (u^n)_2 = \sum_{m=0}^{\infty} U^n_{ml,2} \sin ml\theta, \quad n = 0,\, l, 2l, \ldots . \tag{59}$$

One such pair of modes exists for every $n = 0,\, l, 2l, \ldots$, where n indicates the dominant nodal diameter component (as it does for the mode types to follow). These modes exist for even or odd l. For even l, a second pair of modes, each with distinct natural frequency, exists for every $n = 1/2, 3l/2, 5l/2, \ldots$:

$$(u^n)_1 = \sum_{m=0}^{\infty} U^n_{ml+(l/2),1} \cos\left(ml + \frac{l}{2}\right)\theta, \quad (u^n)_2 = \sum_{m=0}^{\infty} U^n_{ml+(l/2),2} \sin\left(ml + \frac{l}{2}\right)\theta, \quad n = \frac{l}{2}, \frac{3l}{2}, \frac{5l}{2}, \ldots . \tag{60}$$

All split natural frequency modes are of the form (59) or (60). For example, with $l = 4$, representative modes of the form (59) and (60) are

$$(u^4)_1 = U^4_{0,1} + U^4_{4,1} \cos 4\theta + U^4_{8,1} \cos 8\theta + \ldots, \tag{61}$$

$$(u^2)_1 = U^2_{2,1} \cos 2\theta + U^2_{6,1} \cos 6\theta + U^2_{10,1} \cos 10\theta + \ldots . \tag{62}$$

The degenerate modes have degenerate frequencies and reduce from Eq. (49). They evolve from the n nodal diameter free ring modes where $2n/l \neq$ integer, which implies that n can be written as $n = |jl + s|$, where j is an arbitrary integer and s is one of the integers belonging to $[1, \text{int}((l-1)/2)]$. For a given s in this range, these degenerate modes are arbitrary linear combinations of the following two independent modes:

$$(u^n)_1 = \sum_{m=-\infty}^{\infty} U^n_{ml+s} \cos(ml + s)\theta, \quad (u^n)_2 = \sum_{m=-\infty}^{\infty} U^n_{ml+s} \sin(ml + s)\theta, \quad n = s, l \pm s,\, 2l \pm s, \ldots . \tag{63}$$

with $l = 4$, representative modes of the form (63) are

$$\begin{aligned} u^1 = {} & c_1\left[U^1_1 \cos\theta + U^1_{-3} \cos 3\theta + U^1_5 \cos 5\theta + U^1_{-7} \cos 7\theta + \ldots\right] \\ & + c_2\left[U^1_1 \sin\theta - U^1_{-3} \sin 3\theta + U^1_5 \sin 5\theta - U^1_{-7} \sin 7\theta + \ldots\right], \end{aligned} \tag{64}$$

$$u^3 = c_1\left[U_1^3\cos\theta + U_3^3\cos 3\theta + U_5^3\cos 5\theta + U_7^3\cos 7\theta + \ldots\right] + c_2\left[-U_{-1}^3\sin\theta + U_3^3\sin 3\theta - U_{-5}^3\sin 5\theta + U_7^3\sin 7\theta + \ldots\right], \tag{65}$$

where c_1 and c_2 are arbitrary.

When each support has only one spring ($\alpha = 0$ or $\pi/2$), some of the distinct modes have only a single nodal diameter component. These are called *ring modes*. Their natural frequencies are the same as for the corresponding nodal diameter mode for a free ring. When each support has only one tangential spring ($\alpha = 0$), the modes governed by the first of Eqs. (59) and (60) devolve into the ring modes

$$(u^n)_1 = \frac{1}{\sqrt{\pi(1+n^2)}}\cos n\theta, \quad \begin{array}{ll} n = l, 2l, \ldots & \text{for odd } l, \\ n = l/2,\ \ l, 3l/2, \ldots & \text{for even } l. \end{array} \tag{66}$$

Similarly, when each support has only one radial spring ($\alpha = \pi/2$), the modes governed by the second of Eqs. (59) and (60) devolve into the ring modes

$$(u^n)_2 = \frac{1}{\sqrt{\pi(1+n^2)}}\sin n\theta, \quad \begin{array}{ll} n = l, 2l, \cdots & \text{for odd } l, \\ n = l/2,\ l, 3l/2\,, \cdots & \text{for even } l. \end{array} \tag{67}$$

Of all split modes of a ring having identical, equally spaced supports with one spring at each support, half are ring modes and the others are modes of the form $(u^n)_1$ ($\alpha = \pi/2$) or $(u^n)_2$ (for $\alpha = 0$) governed by Eqs. (59) and (60).

4.3. Effect of support number

Fig. 5 shows the relationship between natural frequencies and number of supports obtained by the Galerkin method. All natural frequencies are degenerate for the free ring, and they all split for one or two springs. Fig. 5 confirms the natural frequency splitting rule for rings with l equally spaced springs: when the nodal diameter n and the number of supports l satisfies $n = ml/2$ for even l or $n = ml$ for odd l ($m = 1,2,3,\ldots$), then the natural frequencies split; otherwise they do not. For split modes, the split modes with smallest nodal diameter ($m = 1$) have the largest difference between split natural frequencies. For a given l, the maximum discrepancy between

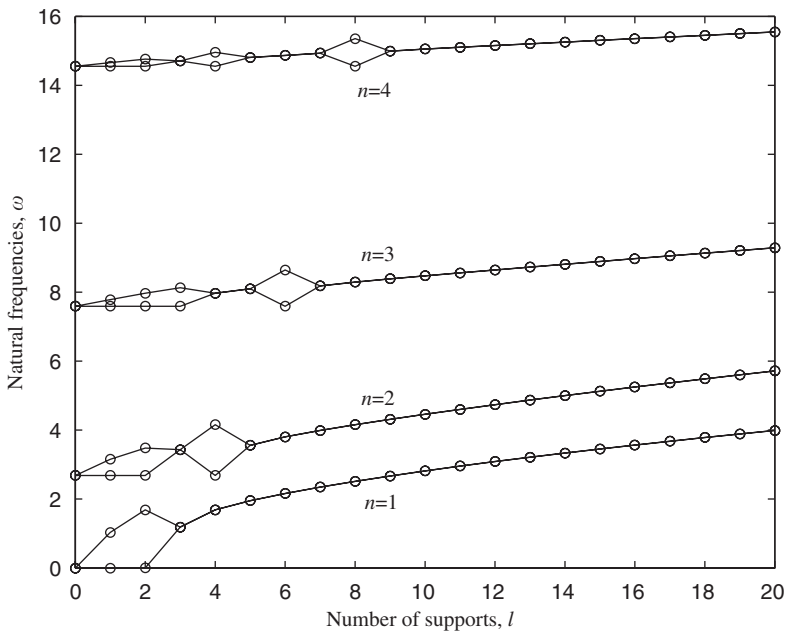

Fig. 5. Natural frequencies versus number of supports (equally spaced) with $\varepsilon = 500$, $\alpha = \pi/2$, $\beta = 0$.

split natural frequencies occurs for $n = 1/2$ for even l and $n = l$ for odd l. For a given n nodal diameter mode, the maximum difference between split natural frequencies always occurs for $l = 2n$.

4.4. Effect of stiffness

The natural frequencies and vibration modes of rings on radial springs were investigated by Allaei et al. [14], which is a special case of the present model with $\alpha = \pi/2$, $\beta = 0$. In this paper, radial springs, tangential springs and their combination are considered. As an example, the dynamic characteristics of a ring with four elastic springs are presented. Fig. 6 shows the natural frequency dependence on stiffness for equally spaced radial or tangential springs ($\beta = 0$). There is a range for each mode where the associated natural frequency is sensitive to spring stiffness, whether radial or tangential. The number of supports l determines the sensitivity of each mode (as discussed in Fig. 5). Comparison of the dashed and solid lines for the same mode shows that tangential stiffness and radial stiffness dominate in different ranges. For small stiffness, the effect of radial springs is stronger than that of tangential springs, while tangential springs are more dominant for high stiffness. For purely radial springs, a rigid body rotational mode ($n = 0$) always exists. When the supports have tangential components, this natural frequency is no longer zero, and its mode shape is contaminated with other nodal diameter modes according to Eq. (56).

As seen in Fig. 6, some natural frequency loci cross each other while others veer away. For example, the loci (solid line) of $n = 3$ and 5 veer away as they approach each other. This is because the three and five nodal diameter modes have the same mode components as they both contain 1,3,5,7,… nodal diameter components, which creates strong coupling of the two modes in the veering region.

Fig. 7 reveals the effects of stiffness on vibration modes from the Galerkin solution. The first eight modes are shown for four identical, equally spaced radial springs with $\varepsilon = 10$, 100, 1000. The vibration modes for $\varepsilon = 1000$ are close to the modes of a ring with rigid springs. Vibration modes with repeated natural frequencies are always heavily contaminated by other numbers of nodal diameters, much more so than for split natural frequency modes, as predicted by perturbation. The contamination is the same for each mode in a repeated natural frequency pair, while a split natural frequency pair has different contamination in each split mode. When the supports are radial springs, one split mode is exactly the free ring vibration mode with no

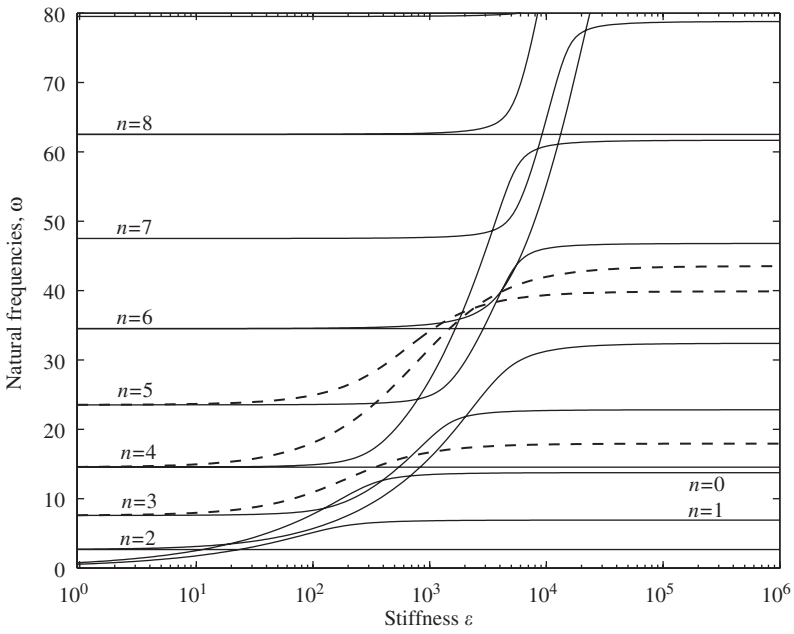

Fig. 6. Natural frequencies for varying spring stiffness ε with $l = 4$, $\beta = 0$ by the Galerkin method. Solid lines denote natural frequencies for tangential stiffness springs ($\alpha = 0$), dashed lines denote natural frequencies for radial springs ($\alpha = \pi/2$).

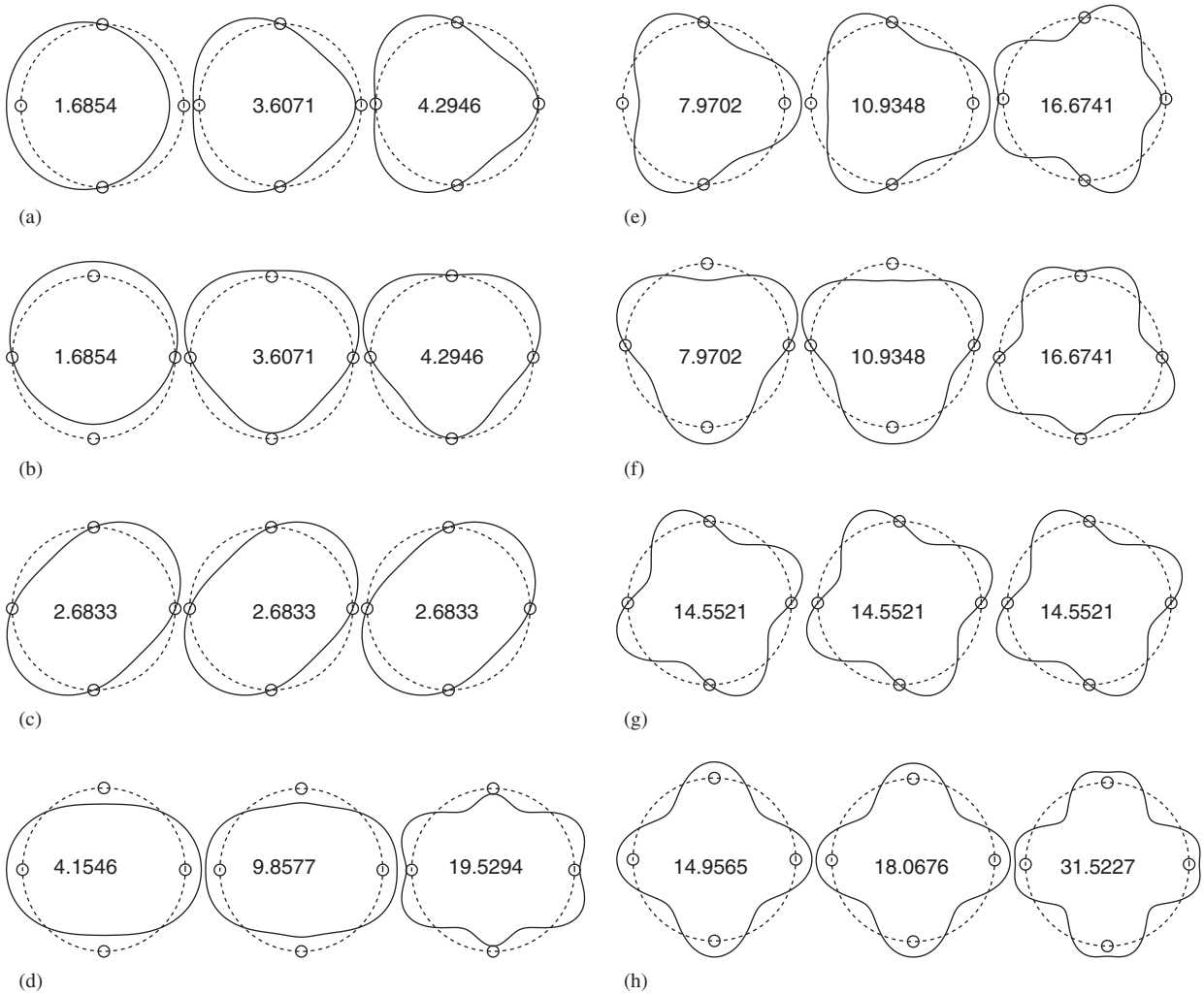

Fig. 7. Mode evolution of a ring with four equally spaced springs radial indicated by circles with $\alpha = \pi/2, \beta = 0$ for $\varepsilon = 10$, 100 and 1000: (a–b) 1 nodal diameter mode; (c–d) 2 nodal diameter mode; (e–f) 3 nodal diameter mode; (g–h) 4 nodal diameter mode. The values are natural frequencies.

contamination (see Fig. 7(c, g)), while the other mode suffers significant mode contamination (see Fig. 7(d, h)), as predicted by perturbation.

For rings with equally spaced tangential or radial springs, each natural frequency is bounded in a specific range as the stiffness increases. The upper bound of natural frequency is determined by the mode contamination sequence for the chosen mode. For a given n nodal diameter base mode, if the contamination sequence is $\ldots,n,p,\ldots$, then the natural frequency is bounded according to

$$\bar{\omega}_n \leq \omega_n < \bar{\omega}_p, \tag{68}$$

where $\bar{\omega}_n$ and $\bar{\omega}_p$ are the n and p nodal diameter natural frequencies for a free ring and ω_n is the corresponding natural frequency of a ring with equally spaced springs. In the above example with $l = 4$, the natural frequencies are bounded as: $\bar{\omega}_0 \leq \omega_0 < \bar{\omega}_4$, $\bar{\omega}_1 \leq \omega_1 < \bar{\omega}_3$, $\bar{\omega}_2 \leq \omega_2 < \bar{\omega}_6$, $\bar{\omega}_3 \leq \omega_3 < \bar{\omega}_5$, and so on.

5. Vibration of rings on unequally spaced spring supports

The ring gear of a planetary gearset with unequally spaced planets can be modeled as a ring with several unequally spaced spring supports. Ring-planet gear tooth meshes are modeled as elastic springs due to tooth

compliance. As a concrete example of a ring with unequally spaced spring supports, the dynamic characteristics of the ring gear in a US Army OH-58 Kiowa helicopter planetary gear are studied. Ring gear parameters and material properties are listed in Table 3. The mesh stiffnesses between the planets and the ring gear are modeled as four unequally spaced springs located at $\theta_1 = 0$, $\theta_2 = 32\pi/63$, $\theta_3 = \pi$ and $\theta_4 = 95\pi/63$ with $\alpha = \pi/2$ and $\beta = 90^\circ - 24.6^\circ$, where 24.6° is the pressure angle. The mesh stiffness is $k = 3.237 \times 10^7$ N/m and the ring bending stiffness is $k_{\text{bend}} = EJ/r^3(1-\nu^2) = 6.0025 \times 10^5$ N/m, so the nondimensional mesh stiffness is $\varepsilon = 53.9279$. The dimensional natural frequencies are found from $\omega_{\text{dim}} = 1266.8\omega$.

When the springs are unequally spaced, the natural frequencies and vibration modes change significantly. Table 4 compares natural frequencies for the unequally and equally spaced cases. All natural frequencies split for rings with asymmetric springs. The modes are shown in Fig. 8. The first two modes shown in Fig. 8 correspond to the two nodal diameter base mode with contamination from the 0, 4, 6, … nodal diameter components.

Table 3
Ring gear parameters and material properties of OH-58

Mass	2.35 kg	Bending stiffness	$k = 3.237 \times 10^7$ N/m
Ring radius	$r = 0.014415$ m	Young's Modulus	$E = 2.0717 \times 10^{11}$ N/m
Ring thickness	$h = 0.01551$ m	Poisson's ratio	$\nu = 0.3$
Face width	$b = 0.0254$ m	Pressure Angle	24.6°

Table 4
Comparison of dimensionless natural frequencies for an elastic ring with four equally and Unequally spaced springs with $\varepsilon = 53.9279$

Natural frequency	ω_1	ω_2	ω_3	ω_4	ω_5	ω_6	ω_7	ω_8
Unequally spaced	2.1469	2.6952	3.1769	3.3201	7.2362	9.2249	9.4470	14.5577
Equally spaced	2.1560	2.6833	3.2477	3.2477	7.2401	9.3367	9.3367	14.5521

Unequally spaced springs are located at $\theta_1 = 0$, $\theta_2 = 32\pi/63$, $\theta_3 = \pi$ and $\theta_4 = 95\pi/63$.

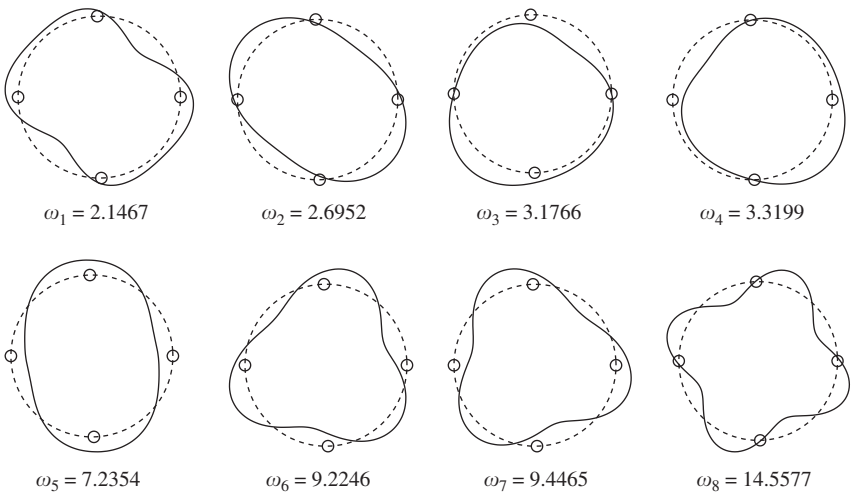

Fig. 8. Modes of a ring on four unequally spaced springs with $\alpha = \pi/2$, $\beta = 65.4^\circ$, and $\varepsilon = 53.9279$. Unequally spaced springs are located at $\theta_1 = 0$, $\theta_2 = 32\pi/63$, $\theta_3 = \pi$, and $\theta_4 = 95\pi/63$.

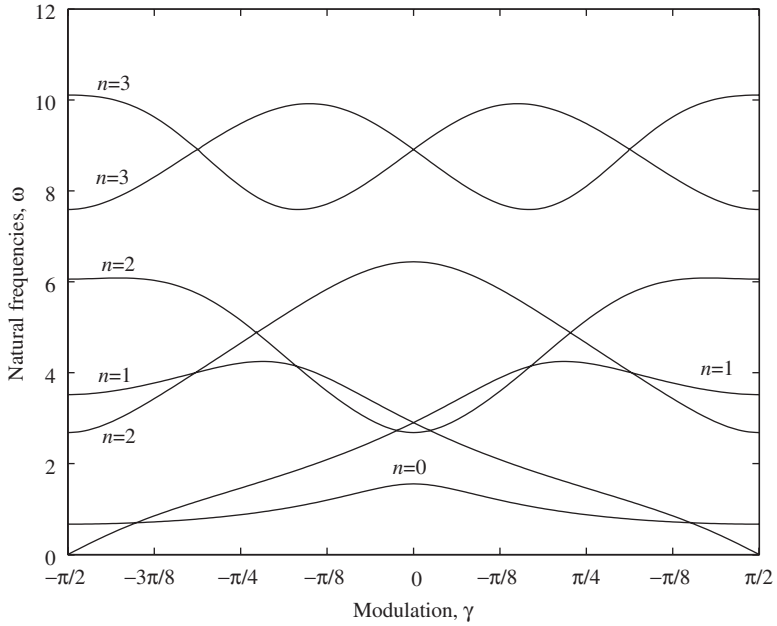

Fig. 9. Natural frequencies for varying modulation γ with $l = 4$, $\alpha = \pi/2$, $\beta = 65.4^\circ$, and $\varepsilon = 53.9279$.

In planetary gears with unequally spaced planets, planet pairs typically lie on diameters, although these diameters are not equally spaced. This is done for load sharing and bearing force considerations. For four planets, the locations of the planets can be represented as $\theta_1 = 0$, $\theta_2 = \pi/2 + \gamma\,\theta_3 = \pi$, $\theta_4 = 3\pi/2 + \gamma$ with γ being a modulation of the equally spaced springs. The influence of modulation γ on natural frequencies is shown in Fig. 9. When $\gamma = \pm\pi/2$, the system is equivalent to rings having two equally spaced springs (the stiffness is doubled at each support). When $\gamma = 0$, the equally spaced case is recovered. According to the natural frequency splitting rule of rings on equally spaced springs, two loci for each of $n = 1,3,\ldots$ meet at $\gamma = 0$, which corresponds to repeated natural frequencies. As the modulation γ changes from $-\pi/2$ to $\pi/2$ the loci of the n nodal diameter base natural frequency pair cross n times.

6. Vibration of rings on distributed elastic foundation

A distributed elastic foundation is an appropriate model in certain rotor/stator systems or bearings. Consider the foundation stiffness distributions

$$d(\theta) = 1 + \tfrac{1}{4}\cos\theta + \tfrac{1}{4}\sin\,\theta + \sin\,4\theta - \tfrac{1}{3}\cos\,6\theta, \quad e(\theta) = \tfrac{1}{4}d(\theta), \tag{69}$$

with $\beta = 0$. Fourier expansion of $d(\theta)$ ensures that only d_0,d_1,d_4,d_6 and their complex conjugates are nonzero. The Fourier coefficients of $e(\theta)$ have the same properties. The set of nontrivial Fourier coefficient indices is $\Upsilon = \{0, \pm1, \pm4, \pm6\}$. Natural frequency splitting properties at the first and second orders are shown in Table 5. Natural frequencies split at the first order for $n = 3$ because $2n \in \Upsilon$. For $n = 2$, the natural frequency pair splits at first order if either of the individual distribution is considered because $2n \in \Upsilon$, but it remains repeated with both $d(\theta)$ and $e(\theta)$ acting simultaneously due to $d_4 - 4e_4 = 0$. Thus, the combined effects of $d(\theta)$ and $e(\theta)$ neutralize the individual effects. Natural frequencies split at second order for $n = 1, 2, 4, 5, 6$ due to $P_{-n,s}P_{s,n} \neq 0$ for certain number of s, such as when $n = 1$ and $s = -5$, or when $n = 4$ and $s = 0$, both $n - s$ and $-n - s$ belong to Υ. Natural frequencies do not split at either order for $n > 6$. According to the mode contamination rule (39), the s nodal diameter components contaminate the n nodal diameter vibration mode for all s satisfying $s \pm n \in \Upsilon$.

Table 5
Natural frequency splitting for rings having the elastic foundations in Eq. (69).

	$n=1$	$n=2$	$n=3$	$n=4$	$n=5$	$n\geq 6$
β_n	R	S	R	R	R	R
γ_n	S		S	S	S	R

S denotes split natural frequencies, and R denotes repeated natural frequencies.

7. Conclusions

The eigensolutions of rings on a general elastic foundation are derived through perturbation and Galerkin analyses. The main conclusions are

- Closed-form expressions for the natural frequencies and vibration modes of rings on a general elastic foundation are formulated through perturbation. This includes discrete and distributed foundations that vary circumferentially in radial, tangential, or inclined orientations.
- The natural frequency splitting and mode contamination rules are obtained in general, compact forms involving the Fourier coefficients of the elastic foundation stiffness distribution functions. Splitting of the n nodal diameter natural frequency at first-order rule is determined by whether or not the $2n$th Fourier coefficients of the foundation vanish. The n nodal diameter mode of the free ring will be contaminated with an s nodal diameter component if $s\pm n=p$ for any non-zero pth coefficient in the foundation's Fourier expansion.
- For rings with identical, equally spaced springs, all modes are described in closed-form. The effects of the number of springs, spring stiffness, and location of the springs are studied. The influence of the springs on vibration modes is more significant for repeated modes than split modes, while the effect on natural frequencies is more significant for split modes than repeated modes.
- For rings with two sets of orthogonally oriented distributed springs, the combined effects may neutralize the effects of the individual foundations on certain modes.

Appendix A. Eigensolution properties of rings with identical, equally spaced spring supports

We are interested in the natural frequency splitting and mode contamination rules at higher order perturbations for a ring having identical, equally spaced spring supports. The eigensolutions are in terms of Q order perturbations

$$\omega_n^2=\bar{\omega}_n^2+\sum_{j=1}^{Q}\varepsilon^j\sigma_{n,j},\quad u_n=\bar{u}_n+\sum_{j=1}^{Q}\varepsilon^j\varphi_{n,j}. \tag{A.1}$$

Substitution of Eq. (A.1) into the eigenvalue problem (13) and collection of like powers of ε give

$$L\varphi_{n,j}-\bar{\omega}_n^2M\varphi_{n,j}=-L_1\varphi_{n,j}+\sum_{m=1}^{j}\sigma_{n,m}M\varphi_{n,j-m},\quad j=1,2,\ldots,Q. \tag{A.2}$$

The natural frequency splitting rule and the mode contamination rule has been obtained at first order perturbation. When $2n/l=\text{int}$,the natural frequencies split at the first order; when $2n/l\neq\text{int}$, the natural frequencies remain repeated at first order. The eigensolutions of the second-order perturbation are governed by Eqs. (34) and (37). For $2n/l\neq\text{int}$, $n-s$ and $-n-s$ cannot simultaneously be integer multiples of l because their difference is $2n$. This and (47) indicate

$$d_{s-n}d_{-s-n}=0,\ d_{s-n}e_{-s-n}=0,\ e_{s-n}e_{-s-n}=0. \tag{A.3}$$

Letting $f^1 = d(\theta)$ and $f^2 = e(\theta)$, Eq. (A.3) is written in a simple form as

$$f^i_{s-n} f^j_{-s-n} = 0,\ i,j = 1,2. \tag{A.4}$$

According to Eq. (A.4), $P_{-n,s}P_{s,n} = 0$ for all s, so the natural frequencies do not split at second order. The second-order eigenfunction perturbation $\varphi_{n,2}$ (η_n in the main text) is

$$\varphi_{n,2} = \eta_n = \sum_{t\neq\pm n}\sum_{s\neq\pm n} \frac{r_{n,s}P_{st}e^{it\theta}}{(1+t^2)(\bar{\omega}_n^2 - \bar{\omega}_t^2)}, \tag{A.5}$$

where $r_{n,s}$ and P_{st} are defined in Eqs. (31) and (32). Eq. (A.5) yields the same mode contamination rule as Eq. (56).

The solvability conditions of the third order perturbation yield

$$\sigma_{n,3}\mathbf{a}_n = \begin{bmatrix} \sum_{t\neq\pm n}\sum_{s\neq\pm n} c_3 P_{n,s}P_{s,t}P_{t,n} & \sum_{t\neq\pm n}\sum_{s\neq\pm n} c_3 P_{-n,s}P_{s,t}P_{t,n} \\ \sum_{t\neq\pm n}\sum_{s\neq\pm n} c_3 P_{n,s}P_{s,t}P_{t,-n} & \sum_{t\neq\pm n}\sum_{s\neq\pm n} c_3 P_{-n,s}P_{s,t}P_{t,-n} \end{bmatrix}\mathbf{a}_n, \tag{A.6}$$

$$c_3 = \frac{C_{n,s}}{(1+t^2)(\bar{\omega}_t^2 - \bar{\omega}_n^2)}, \tag{A.7}$$

where $C_{n,s}$ is defined in the second of Eq. (31). The two diagonal terms in Eq. (A.6) are identical and real, and the two off diagonal terms are complex conjugate. Consequently,

$$\sigma_{n,3} = \sum_{t\neq\pm n}\sum_{s\neq\pm n} c_3 P_{n,s}P_{s,t}P_{t,n} \pm \left| \sum_{t\neq\pm n}\sum_{s\neq\pm n} c_3 P_{-n,s}P_{s,t}P_{t,-n} \right|. \tag{A.8}$$

One can prove that $s-n$, $t-s$ and $-t-n$ cannot simultaneously be integer multiples of l for $2n/l \neq \text{int}$. A similar equation as Eq. (A.3) is obtained:

$$f^i_{s-n} f^j_{t-s} f^k_{-t-n} = 0, \quad i,j,k = 1,2. \tag{A.9}$$

Thus, the second term of Eq. (A.8) vanishes, and the natural frequencies remain repeated at third order. Comparison of Eqs. (37) and (A.8) indicates that the eigenvalue expressions have the same pattern. For each higher order of perturbation, the number of the summation increases by one. Thus, one can anticipate the eigenvalue expression for the Qth order perturbation:

$$\sigma_{n,Q} = \sum_{t\neq\pm n}\sum_{s\neq\pm n}\cdots\sum_{w\neq\pm n}\sum_{y\neq\pm n} c_M \underbrace{P_{n,s}P_{s,t}\cdots P_{w,y}P_{y,n}}_{Q} \pm \left| \sum_{t\neq\pm n}\sum_{s\neq\pm n}\cdots\sum_{y\neq\pm n} c_M \underbrace{P_{n,s}P_{s,t}\cdots P_{w,y}P_{y,-n}}_{Q} \right|. \tag{A.10}$$

Similarly, one can show that

$$f^i_{s-n} f^j_{t-s}\cdots f^o_{y-w} f^z_{-y-n} = 0, \quad i,j,\ldots,o,z = 1,2. \tag{A.11}$$

Eq. (A.11) guarantees that the second term of Eq. (A.10) vanishes, so the natural frequencies are still repeated at the Qth order of perturbation for $2n/l \neq \text{int}$. The natural frequency splitting rule obtained from the first order holds for any order of perturbation. Similar conclusion can be drawn for the mode contamination rule.

References

[1] H.N. Ozguven, D.R. Houser, Mathematical-models used in gear dynamics—a Review, *Journal of Sound and Vibration* 121 (1988) 383–411.

[2] J. Lin, R.G. Parker, Analytical characterization of the unique properties of planetary gear free vibration, *Journal of Vibration and Acoustics* 121 (1999) 316–321.

[3] G.D. Bibel, S.K. Reddy, M. Savage, Effect of rim thickness on spur gear bending stress, NASA Technical Memorandum 104388, 1991.

[4] C.A. Brazakis, D.R. Houser, Finite element and experimental analysis of the effects of thin-rimmed gear geometry on spur gear fillet stresses, *International Gearing Conference*, Newcastle upon Tyne, UK, 1994, pp. 41–46.
[5] T. Chiang, R.H. Badgley, Reduction of vibration and noise generated by planetary ring gears in helicopter aircraft transmissions, *Journal of Engineering for Industry* 95 (1973) 1149–1158.
[6] A. Kahraman, A.A. Kharazi, M. Umrani, A deformable body dynamic analysis of planetary gears with thin rims, *Journal of Sound and Vibration* 262 (2003) 752–768.
[7] S.S. Rao, V. Sundararajan, In-plane flexural vibration of circular rings, *Journal of Applied Mechanics, Design Data and Methods* 36 (1969) 620–625.
[8] K.B. Sahay, V. Sundararajan, Vibration of a stiffened ring considered as a cyclic structure, *Journal of Sound and Vibration* 22 (1972) 467–473.
[9] T.J. McDaniel, Dynamics of Circular Periodic Structures, *Journal of Aircraft* 8 (1971) 143–149.
[10] V.R. Murthy, N.C. Nigam, Dynamic characteristics of stiffened rings by transfer matrix approach, *Journal of Sound and Vibration* 39 (1975) 237–245.
[11] K. Singh, B.L. Dhoopar, Free vibration of circular rings on radial supports, *Journal of Sound and Vibration* 65 (1979) 297–301.
[12] A.K. Mallik, D.J. Mead, Free vibration of thin circular rings on periodic radial supports, *Journal of Sound and Vibration* 54 (1977) 13–27.
[13] F.M. Detinko, Free vibration of a thick ring on multiple supports, *International Journal of Engineering Science* 27 (1989) 1429–1438.
[14] D. Allaei, W. Soedel, T.Y. Yang, Natural frequencies and modes of rings that deviate from perfect axisymmetry, *Journal of Sound and Vibration* 111 (1986) 9–27.
[15] R.C. Yu, C.D. Mote Jr., Vibration and parametric excitation in asymmetric circular plates under moving loads, *Journal of Sound and Vibration* 119 (1987) 409–427.
[16] J.G. Tseng, J.A. Wickert, On the vibration of bolted plate and flange assemblies, *Journal of Vibration and Acoustics* 116 (1994) 468–473.
[17] R.G. Parker, C.D. Mote Jr., Exact perturbation for the vibration of almost annular or circular plates, *Journal of Vibration and Acoustics* 118 (1996) 436–445.
[18] R.G. Parker, C.D. Mote Jr., Exact boundary condition perturbation solutions in eigenvalue problems, *Journal of Applied Mechanics* 63 (1996) 128–135.
[19] R.G. Parker, C.D. Mote Jr., Exact boundary condition perturbation for eigensolutions of the wave equation, *Journal of Sound and Vibration* 211 (1998) 389–407.
[20] M. Kim, J. Moon, J.A. Wickert, Spatial modulation of repeated vibration modes in rotationally periodic structures, *Journal of Vibration and Acoustics* 122 (2000) 62–68.
[21] J.Y. Chang, J.A. Wickert, Measurement and analysis of modulated doublet mode response in mock bladed disks, *Journal of Sound and Vibration* 253 (2002) 379–400.
[22] J.Y. Chang, J.A. Wickert, Response of modulated doublet modes to travelling wave excitation, *Journal of Sound and Vibration* 242 (2001) 69–83.
[23] T.E. Lang, Vibration of thin circular rings, part 2. Modal functions and eigenvalues of constrained semicircular rings, *JPL Technical Report* (1963) 32–261.
[24] C.H.J. Fox, A simple theory for the analysis and correction of frequency splitting in slightly imperfect rings, *Journal of Sound and Vibration* 142 (1990) 227–243.
[25] R.G. Parker, C.D. Mote Jr., Vibration and coupling phenomena in asymmetric disk-spindle systems, *Journal of Applied Mechanics* 63 (1996) 953–961.
[26] J.Y. Chang, J.A. Wickert, Measurement and analysis of modulated doublet mode response in mock bladed disks, *Journal of Sound and Vibration* 250 (2002) 379–400.